



Biosorption of methylene blue by natural and chemical modified wheat straw in fixed-bed column

Xiaofeng Ren, Xiaona Zhang, Lijun Zhang, Runping Han*

School of Chemistry and Molecular Engineering, Zhengzhou University, No 100 of Kexue Road, Zhengzhou 450001, P.R. China

Tel. +86 371 67781757; Fax: +86 371 67781556; email: rphan67@zzu.edu.cn

Received 12 September 2012; Accepted 4 October 2012

ABSTRACT

Adsorption of methylene blue (MB) from aqueous solution was studied by natural wheat straw (NWS) and modified wheat straw (MWS) with citric acid in fixed-bed column. The experiments were conducted to investigate the effects of the bed depth, the flow rate, and the influent concentration of MB. The column data were fitted by the Thomas model and Yan model using nonlinear regressive analysis, while bed depth/service time analysis (BDST) model was applied at different bed depths. The Yan and BDST were found suitable for describing the adsorption process. The exhausted adsorbent was regenerated using hydrogen chloride solution and the adsorbent was reused. The results showed that the adsorption capacity of MWS was higher than NWS and both NWS and MWS can be reused.

Keywords: Wheat straw; Modified wheat straw; Methylene blue; Column adsorption; Model

1. Introduction

Dyes are discharged from various industries, such as textile, paper, cosmetics, plastics, food, and so on. The presence of dyes in wastewater is greatly visible and undesirable even at very low concentrations. Color retards light penetration, impedes photosynthetic activity, and inhibits the development of biota. Currently, considerable attention has been given to the methods for eliminating dyes from wastewater because of their toxic nature and refractory biodegradation. The conventional wastewater treatment methods, such as chemical precipitation, solvent extraction, reverse osmosis, electrolysis, and ion exchange, are not very effective owing to the low biodegradability of dyes, high energy requirement and operational cost, and

incomplete removal [1]. Adsorption technique has a wide variety of applications and has been demonstrated to be a valid and promising process for the treatment of these dye-bearing wastewaters because of its easy operation, insensitivity to toxic or harmful substances, ability to treat concentrated solution of pollutant, and the possibility of reusing the exhausted adsorbent through regeneration [2]. In recent years, the most widely used adsorbent, activated carbon, has good capacity for the removal of dyes. However, the critical challenges of the sorption method are the high price of the adsorbent and difficult regeneration, which increases the cost of wastewater treatment [3–5]. Therefore, attempts have already been made to change this dilemma. For instance, it is preferable to use low-cost materials; agricultural by-products, such as fallen leaves [6], rice husk [7,8], wheat husk [9,10], peanut

*Corresponding author.

husk [11], sawdust [12], bottom ash and de-oiled Soya [13–15]; and durian peel [16] as adsorbents. Some of the low-cost adsorbents were found to be potential and low cost for dealing with colored waste water. The researches have been reviewed [17,18].

In this article, wheat straw was selected as a adsorbent for the removal of methylene blue (MB) from its aqueous solutions because of two factors. Firstly, it contains adequate cellulose; protein; and several functional groups, such as hydroxyl, carboxyl, and amidogen, making the adsorption processes more feasible [19]. Furthermore, wheat is a widely cultured food crop in China. Consequently, the wheat straw was obtained extensively and cheaply as a by-product acquired from agriculture.

As a matter of fact, natural wheat straw (NWS) as an adsorbent is possibly not advantageous for physical and chemical characteristics. Because of poor performance of NWS for MB adsorption, many attempts have been implemented. One of them is chemical modification using citric acid (CA), which was an effect media to enhance the adsorption capacity of NWS for dyes.

Previously in our laboratory, NWS and modified wheat straw (MWS) were used as adsorbents to remove MB and copper ion from solution in batch mode, respectively [19,20]. The results showed that there was higher adsorption capacity for MWS. However, the information obtained from the batch experiments did not apply to continuous operation. The process engineering advantages of a fixed-bed adsorption column with adsorbents offer easy continuous operation and scale up is an important aspect of the adsorption process. But no research was reported about MB adsorption to NWS and MWS in column mode. Therefore, it is imperative to describe dynamic behavior in a fixed-bed column condition.

The research described here was designed to investigate the biosorption behavior of utilization NWS and MWS for the removal of MB from solution in fixed-bed column. The effects of main variables, such as flow rate, influent concentration, and bed depth, on MB adsorption were researched. In order to predict the performance in the column, the experimental data were processed with Thomas model, Yan model, and bed depth/service time model (BDST).

1.1. Thomas model

The Thomas model is used for the description of the breakthrough curve, calculating the maximum solid phase concentration on adsorbent and the adsorption rate constant. The expression by Thomas for an adsorption column is given as follows [21]:

$$\frac{C_t}{C_0} = \frac{1}{1 + \exp(k_{Th}q_0x/v - k_{Th}C_0t)} \quad (1)$$

where q_0 is the adsorption capacity per g of the adsorbent (mg g^{-1}); k_{Th} is the rate constant ($\text{mL min}^{-1} \text{mg}^{-1}$); x is the quality of adsorbent in the column (g); C_0 is the influent MB concentration (mg L^{-1}); C_t is the effluent concentration at any time t (mg L^{-1}); and v is the flow rate (mL min^{-1}). The value of C_t/C_0 is the proportion of effluent and influent MB concentrations.

The kinetic coefficient k_{Th} and the adsorption capacity of the column q_0 can be determined from a plot of C_t/C_0 against t at a given flow rate using nonlinear regression.

1.2. Yan model

Yan model [22,23] is also used to describe column adsorption data. Use of this model can minimize the error resulting from the use of the Thomas model, especially at lower or higher time periods of the breakthrough curve. The expression is given as:

$$\frac{C_t}{C_0} = 1 - \frac{1}{1 + (vt/b)^a} \quad (2)$$

where a and b are the constants of Yan model, respectively.

1.3. The BDST analysis model

The BDST model is based on physically measuring the capacity of the bed at different breakthrough values. The BDST model works well and provides useful modeling equations for the changes of system parameters [23]. A modified form of the equation that expresses the service time at breakthrough, t , as a fixed function of operation parameters is BDST model:

$$t = \frac{N_0}{C_0F}Z - \frac{1}{K_aC_0} \ln\left(\frac{C_0}{C_t} - 1\right) \quad (3)$$

where C_t = effluent concentration of solute in the liquid phase (mg L^{-1}); C_0 = initial concentration of solute in the liquid phase (mg L^{-1}); F = influent linear velocity (cm min^{-1}); N_0 = adsorption capacity (mg L^{-1}); K_a = rate constant in BDST model ($\text{L mg}^{-1} \text{min}^{-1}$); t = time (min); and Z = bed depth of column (cm).

A plot of t vs. bed depth, Z , should yield a straight line where N_0 and K , the adsorption capacity and rate constant, respectively, can be evaluated.

A simplified form of the BDST model is:

$$t = aZ - b \quad (4)$$

where

$$a = \frac{N_0}{C_0 F}, \quad b = \frac{1}{K_a C_0} \ln \left(\frac{C_0}{C_t} - 1 \right) \quad (5)$$

The slope constant for a different flow rate can be directly calculated by Eq. (6) [23]:

$$a' = a \frac{F}{F'} = a \frac{v}{v'} \quad (6)$$

where a and F are the old slope and influent linear velocity, respectively, and a' and F' are the new slope and influent linear velocity. As the column used in experiment has the same diameter, the ratio of original (F) and the new influent linear velocity (F') and the original flow rate (v) and the new flow rate (v') is equal.

For other influent concentrations, the desired equation is given by a new slope and a new intercept is given by:

$$a' = a \frac{C_0}{C'_0} \quad (7)$$

$$b' = b \cdot \frac{C_0}{C'_0} \cdot \frac{\ln(C'_0 - 1)}{\ln(C_0 - 1)} \quad (8)$$

where b' and b are the new and old intercepts, respectively, C'_0 and C_0 are the new and old influent concentrations, respectively.

1.4. Error analysis

Nonlinear regressive method was used in this paper, which can improve the accuracy significantly [24–26]. The relative mathematical formula is:

$$SS = \sum (y_e - y_c)^2 \quad (9)$$

where y_e and y_c are the experimental and calculated values according to the model, respectively, and N is the number of the experimental point. In order to confirm the best fit model for the adsorption system, it is necessary to analyze the data using SS, combined the values of determined coefficient (R^2). The experimental data were analyzed by software of Origin 7.0.

2. Materials and methods

2.1. Preparation of NWS

Fresh biomass of wheat straw was obtained from local countryside of Luoyang City, China. The

collected biomaterial was seriously washed with distilled water several times to remove all the dirt particles, and dried in an oven at 50°C. Dry wheat straw was crushed into powder and screened through a set of sieves to get geometrical sizes of 20–40 mesh, which produced a uniform material for the adsorption tests, and then conserved in the desiccator for use.

2.2. Preparation of MWS

The process was similar to previous study [19]. Ground wheat straw was mixed with 0.6 mol L⁻¹ CA at the ratio of 1:12 (straw/acid, w/v) and stirred for 30 min at 20°C. Then the samples were poured into stainless steel plate and dried for 24 h at 80°C in the oven. Then the esterification reaction was conducted for 1.5 h at 120°C. When the wheat straw cooled, it was rinsed using distilled water to remove unreacted CA. Afterwards, the solution was filtrated until there was no precipitation when 0.1 mol L⁻¹ of lead nitrate was added. After filtration, MWS was suspended in 0.1 mol L⁻¹ NaOH solution at suitable ratio and stirred for 60 min, followed by washing thoroughly with distilled water to remove residual alkali, next dried at 50°C for 24 h, and preserved in a desiccator for use.

2.3. MB solution

The stock solutions of MB (500 mg L⁻¹) were prepared in distilled water. All working solutions were prepared by diluting the stock solution with distilled water to the needed concentration. The solution pH was near 7.5 and not adjusted during experiments.

2.4. Adsorption studies

Fixed-bed column adsorption experiments were carried out using NWS and MWS packed into a glass column (1.0 cm inner diameter and 25 cm in height) with a bed depth of 6, 8.5, and 11 cm, respectively. The experiments were conducted by pumping a MB solution in down flow mode through the fixed-bed with a peristaltic pump. The temperatures of all experiments were 293 K. Samples were collected at regular intervals in the adsorptive process. The concentration of MB in the effluent was analyzed using a UV spectrophotometer (Shimadzu Brand UV-3000) by monitoring the absorbance changes at a wavelength of maximum absorbance (668 nm).

The concentration of MB desorbed from MB-loaded adsorbent in column by 0.1 mol L⁻¹ hydrogen chloride solution also was analyzed and the regenerated column was reused to adsorb MB for NWS and MWS (for column depth 8.5 cm, flow rate 5.6 mL min⁻¹, and MB concentration 80 mg L⁻¹).

3. Result and discussion

3.1. The effect of different bed depths on breakthrough curves

The breakthrough curves at different bed depths for NWS and MWS are shown in Fig. 1, respectively.

From Fig. 1, the trends of curves of NWS are similar to MWS with bed depth change. As the bed height increases, MB had more time to contact with rice husk that resulted in higher removal efficiency of MB ions in column. So the higher bed column results in a decrease in the solute concentration in the effluent at the same time. The slope of breakthrough curve decreased with increasing bed height, which resulted in a broadened mass transfer zone [27].

3.2. The effect of flow rate on breakthrough curves

The breakthrough curves at various flow rates are shown in Fig. 2.

It was shown that breakthrough generally occurred faster with higher flow rate for both NWS and MWS.

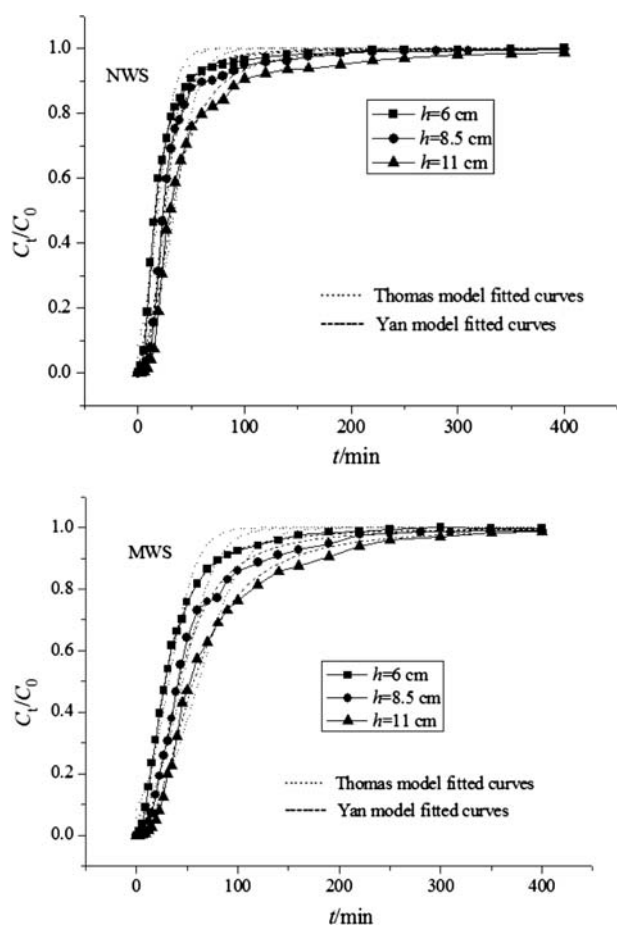


Fig. 1. Breakthrough curves at different bed depths ($C_0 = 80 \text{ mg L}^{-1}$ and $v = 5.6 \text{ mL min}^{-1}$).

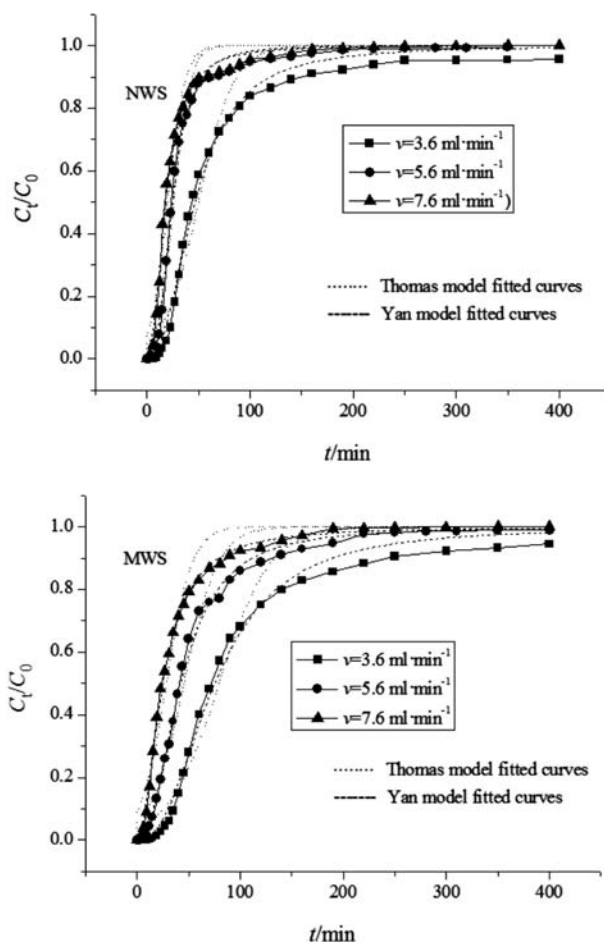


Fig. 2. Breakthrough curves at various flow rates ($Z = 8.5 \text{ cm}$, and $C_0 = 80 \text{ mg L}^{-1}$).

Breakthrough time reaching saturation was increased significantly with a decrease in the flow rate. At a low rate of influent, MB had more time to contact with rice husk than that resulted in higher removal of MB ions in column [27].

3.3. Effect of influent MB concentration on breakthrough curves

The effect of influent MB concentration on the shape of the breakthrough curves is shown in Fig. 3.

It is illustrated that the breakthrough time decreased with increasing influent MB concentration. At lower influent MB concentrations, breakthrough curves were dispersed and breakthrough occurred slower. As influent concentration increased, sharper breakthrough curves were obtained. This can be explained by the fact that more adsorption sites were being covered as the MB concentration increasing. The larger the influent concentration, the steeper is the slope of breakthrough curve and smaller is the

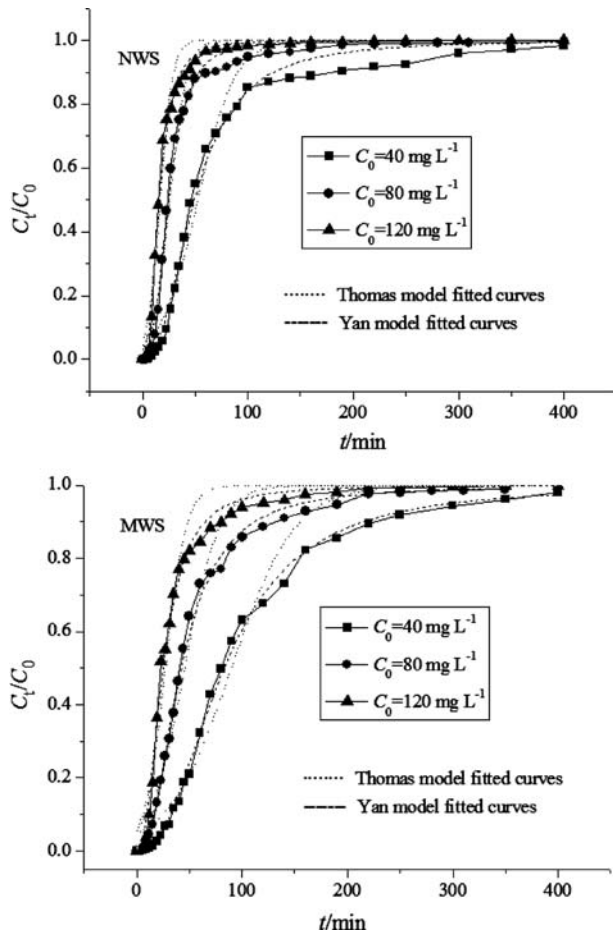


Fig. 3. Breakthrough curves at different influent concentrations ($Z=8.5$ cm and $v=5.6$ mL min⁻¹).

breakthrough time. These results demonstrate that the change of concentration gradient affects the saturation rate and breakthrough time or, in other words, the diffusion process is concentration dependent [27].

Compared to breakthrough curves (Figs. 1–3) at same condition (same about bed depth, flow rate, and copper concentration) between NWS and MWS, it can be seen that the breakthrough time and exhausted time of MWS are longer than those of NWS, respectively. These results showed that MWS had more adsorption capacity for copper ions than NWS. This was also confirmed by the adsorption in batch mode [19,20].

3.4. Modeling of column study results

Modeling of data available from column studies facilitates scale-up potential. To describe the column breakthrough curves obtained at different bed heights, flow rates, and inlet MB concentrations, three models were used. These included the Thomas, Yan, and BDST models.

3.4.1. Thomas model

Thomas model was applied to the experimental data at different conditions. A nonlinear regression analysis was used on each set of data to determine the Thomas model parameters of q_0 and k_{Th} . The determined coefficients and the SS were also obtained using nonlinear regression analysis according to the Eq. (1). The results are listed in Table 1. The fitted

Table 1
Thomas model parameters at different conditions

C_0 (mg L ⁻¹)	v (mL min ⁻¹)	Z (cm)	q_{exp} (mg g ⁻¹)	q_0 (mg g ⁻¹)	k_{Th} (mL min ⁻¹ mg ⁻¹)	R^2	SS
NWS							
80	5.6	6	41.2	30.1	1.56	0.970	0.00331
80	5.6	8.5	40.5	29.2	1.62	0.979	0.00298
80	5.6	11	44.6	29.6	1.10	0.981	0.00561
80	3.6	8.5	52.5	35.9	0.741	0.960	0.00601
80	7.6	8.5	42.9	30.8	1.67	0.968	0.00373
40	5.6	8.5	42.6	29.4	1.45	0.964	0.00538
120	5.6	8.5	36.4	28.5	1.47	0.974	0.00313
MWS							
80	5.6	6	65.5	50.3	0.937	0.976	0.00305
80	5.6	8.5	67.8	50.9	0.769	0.970	0.00443
80	5.6	11	69.8	53.2	0.578	0.963	0.00553
80	3.6	8.5	77.3	57.2	0.510	0.961	0.00573
80	7.6	8.5	58.7	43.0	1.02	0.965	0.00442
40	5.6	8.5	61.5	50.3	0.839	0.971	0.00422
120	5.6	8.5	62.9	45.7	0.871	0.967	0.00454

Table 2
Yan model parameters at different conditions

C_0 (mg L ⁻¹)	v (mL min ⁻¹)	Z (cm)	a	b (mL)	R^2	SS
NWS						
80	5.6	6	2.08	469	0.998	0.00019
80	5.6	8.5	2.83	691	0.995	0.00068
80	5.6	11	2.34	902	0.992	0.0011
80	3.6	8.5	2.32	839.5	0.992	0.00110
80	7.6	8.5	2.18	693.5	0.996	0.00047
40	5.6	8.5	2.38	1,385	0.992	0.00108
120	5.6	8.5	2.64	441.5	0.995	0.00055
MWS						
80	5.6	6	1.99	791.5	0.999	0.00004
80	5.6	8.5	2.35	1,183	0.997	0.00043
80	5.6	11	2.22	1,582.5	0.996	0.00062
80	3.6	8.5	2.38	1,358.5	0.993	0.00096
80	7.6	8.5	1.91	952.5	0.998	0.00021
40	5.6	8.5	2.31	2,327	0.998	0.00026
120	5.6	8.5	2.33	702.5	0.994	0.00078

curves are also shown in Figs. 1–3, respectively. They were all with higher determined coefficients (R^2) ranging (larger 0.96) and lower SS (smaller than 0.00610) from Table 1.

From Table 1, with flow rate increasing, the value of q_0 for NWS and MWS decreased, but the value of k_{Th} increased. As the bed depth increased, the value of q_0 increased, while the value of k_{Th} decreased for MWS. There were not similar trends with change of MB concentration. Compared to the value of q from experiment and calculation, there was large difference at same condition. Furthermore, the Thomas fitted curves were far to experimental curves, so this model was not better to predict the column behavior.

3.4.2. Yan model

Yan model minimized the error that results from use of the Thomas model, especially with lower and higher breakthrough curve times. Yan model was also used to fit the experimental data and some parameters are listed in Table 2. Relative fitted curves are also presented in Figs. 1–3. From Table 2, there were higher value of R^2 and lower value of SS for both NWS and MWS. Furthermore, the predicted curves and experimental curves were very close at same condition. So, it can be conclude that Yan model can be used to predict the whole breakthrough curves. From Table 2, values of b became larger with bed depth increase, but it became smaller with the increase of flow rate and initial dye concentration, respectively. Other research in our previous study also

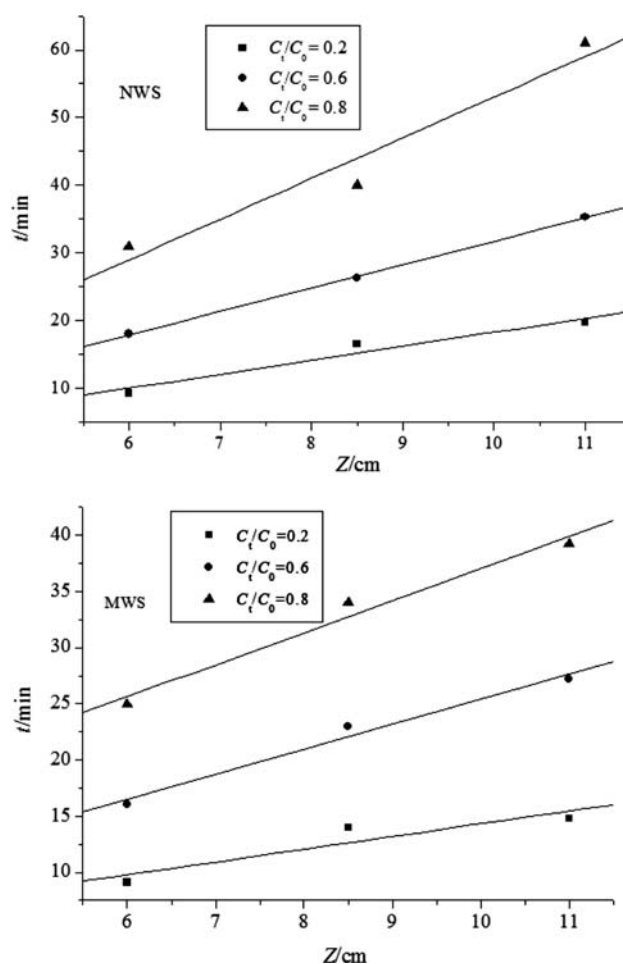


Fig. 4. Isoremoval lines for 0.2, 0.4, and 0.6 breakthrough for different bed depths ($C_0=80$ mg L⁻¹ and $v=5.6$ mL min⁻¹).

found that Yan model was better to predict the breakthrough curves than Thomas model [28–30].

3.4.3. BDST model

The BDST model as a fixed function of operation parameters was on the basis of physically measuring the capacity of the bed at different breakthrough values.

The lines of $t-Z$ at values of C_t/C_0 0.2, 0.6, and 0.8 for NWS and MWS are shown in Fig. 4, respectively. The related constants of BDST according to the slopes and intercepts of lines are listed in Table 3.

From Table 3, it was observed that the adsorption capacity of the bed per unit bed volume, N_0 , increased dramatically, while the rate constant of K_a decreased slightly along with the value of C_t/C_0 increasing. According to the values of R^2 , the rationality of the BDST model for the adsorption processes was identified. Moreover, MWS had more excellent adsorption capacity along with higher values of N_0 , compared with NWS in the same situation.

In addition, the BDST model constants can be used to predict the adsorbent performance for other flow rate and concentration without further process. For instance, the BDST constants gained at flow rate

5.6 mL min⁻¹ and influent concentration 80 mg L⁻¹ were helpful to forecast the adsorbent behavior at higher flow rate of 7.6 mL min⁻¹ and lower influent concentration of 40 mg L⁻¹, respectively. Meanwhile, the corresponding calculated time (t_c) and experimental time (t_e) were demonstrated in Tables 4 and 5, respectively.

It was observed that the values of t_c were similar to the experimental results, which indicated good prediction for the case of changed influent concentration and flow rate. Hence, the BDST model can be available for designing columns over a broad range of flow rate and concentrations at $C_t/C_0=0.2, 0.6,$ and 0.8 , respectively.

In conclusion from Tables 4 and 5, all the results revealed the validity of BDST model for the adsorption of MB onto wheat straw. This model was useful to predict adsorption performance at further experimental situations.

3.5. Regeneration and MB loaded NWS and MWS and reuse

Disposal of the exhausted adsorbent loaded with pollutant creates another environmental problem as it is the hazardous material which pollutes environ-

Table 3

Calculated constants of the BDST model for the adsorption of MB onto NWS and MWS ($C_0=80$ mg L⁻¹ and $v=5.6$ mL min⁻¹)

C_t/C_0	a (min cm ⁻¹)	b (min)	K_a (L mg ⁻¹ min ⁻¹)	N_0 (mg L ⁻¹)	q (mg g ⁻¹)	R^2
<i>MB adsorption onto NWS</i>						
0.2	2.07	2.46	7.05×10^{-3}	928	3.09	0.909
0.6	3.39	2.15	-2.35×10^{-3}	1,518	5.06	0.998
0.8	6.02	7.19	-2.41×10^{-3}	2,698	8.99	0.905
<i>MB adsorption onto MWS</i>						
0.2	4.02	10.7	1.62×10^{-3}	1,799	6.00	0.998
0.6	5.83	0.784	-6.46×10^{-3}	2,614	8.71	0.997
0.8	11.6	14.3	-1.21×10^{-3}	4,197	13.97	0.999

Table 4

Predicted breakthrough time based on the BDST constants for a new flow rate ($v=7.6$ mL min⁻¹)

C_t/C_0	v (mL min ⁻¹)	v' (mL min ⁻¹)	a' (min cm ⁻¹)	b' (min)	t_c (min)	t_e (min)
<i>The adsorption of MB onto NWS ($Z=8.5$ cm, $C_0=80$ mg L⁻¹)</i>						
0.2	5.6	7.6	1.53	2.46	10.5	11.5
0.6	5.6	7.6	2.50	2.15	19.1	20.3
0.8	5.6	7.6	4.44	7.19	30.5	33.8
<i>The adsorption of MB onto MWS ($Z=8.5$ cm, $C_0=80$ mg L⁻¹)</i>						
0.2	5.6	7.6	2.96	10.7	14.4	12.7
0.6	5.6	7.6	4.30	0.784	35.8	31.6
0.8	5.6	7.6	8.55	14.3	54.4	52.3

Table 5

Predicted breakthrough time based on the BDST constants for a new MB concentration ($C_0 = 40 \text{ mg L}^{-1}$)

C_t/C_0	$C_0 \text{ (mg L}^{-1}\text{)}$	$C'_0 \text{ (mg L}^{-1}\text{)}$	$a' \text{ (min cm}^{-1}\text{)}$	$b' \text{ (min)}$	$t_c \text{ (min)}$	$t_e \text{ (min)}$
<i>The adsorption of MB onto NWS ($Z = 8.5 \text{ cm}$, $v = 5.6 \text{ mL min}^{-1}$)</i>						
0.2	80	40	4.14	4.91	30.3	29.7
0.6	80	40	6.78	4.31	53.3	54.5
0.8	80	40	12.1	14.4	88.0	89.6
<i>The adsorption of MB onto MWS ($Z = 8.5 \text{ cm}$, $v = 5.6 \text{ mL min}^{-1}$)</i>						
0.2	80	40	8.03	21.5	46.8	46.2
0.6	80	40	11.7	1.57	97.6	95.9
0.8	80	40	23.2	28.6	159	155

ment. The use of biomass as a potential adsorbent depends not only on the adsorptive capacity, but also on how well the biomass regenerated and reused in the recycling process, especially for modified adsorbent. Regeneration must produce small volume of dye concentrates without significantly damaging the capacity of the adsorbent,

making it reusable in several adsorptions and desorption cycles [30–34].

Desorbed experiments were performed with 0.1 mol L^{-1} hydrogen chloride solution as the desorbed agent at 5.6 mL min^{-1} . Fig. 5 shows the desorbed curves. As shown in Fig. 5, MB was easily desorbed because the desorption nearly completed in less

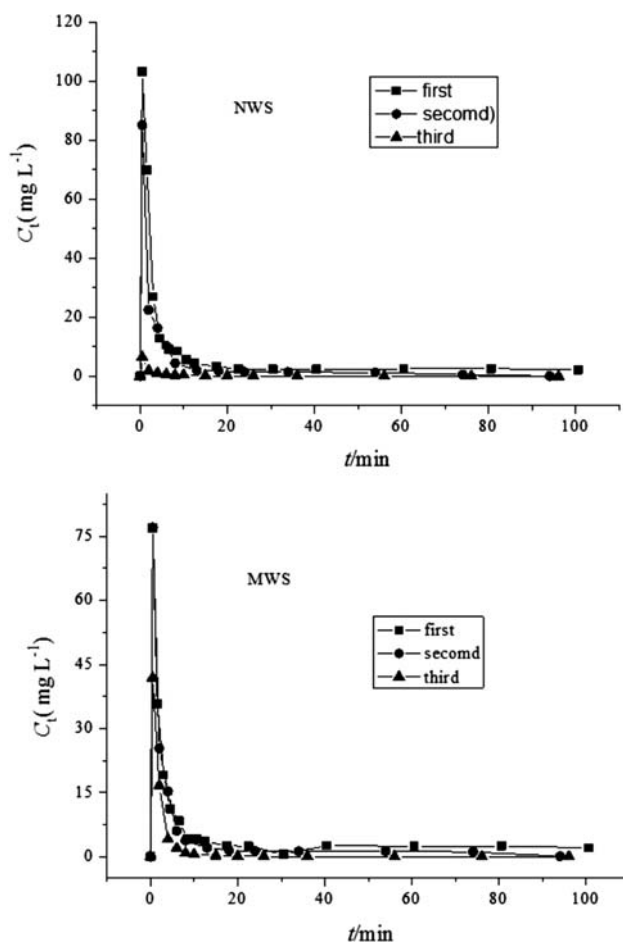


Fig. 5. Elution curves for MB from NWS and MWS column ($Z = 8.5 \text{ cm}$, $C_0 = 80 \text{ mg L}^{-1}$, and $v = 5.6 \text{ mL min}^{-1}$).

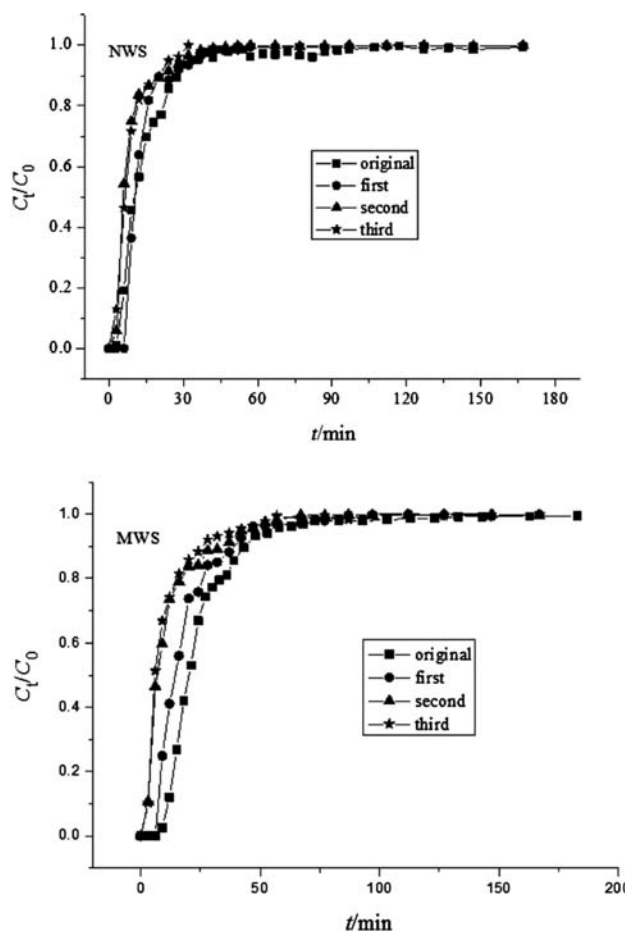


Fig. 6. Adsorption/desorption cycles about MB adsorption onto NWS and MWS column ($Z = 8.5 \text{ cm}$, $C_0 = 80 \text{ mg L}^{-1}$, and $v = 5.6 \text{ mL min}^{-1}$).

than 50 min. Fig. 6 shows the recycles of adsorbed MB by NWS and MWS. The first, second, and third regeneration yields are 68.0, 46.8, and 57.2% for NWS and 57.6, 39.6, and 43.5% for MWS, respectively. The results showed that NWS and MWS can be used repeatedly with losing some adsorption capacity for the removal of MB from solution. Hence, the regeneration and reuse of NWS and MWS was an economical and an efficient method for the removal of MB from water. From the results of desorption and regeneration obtained using HCl solution, ion exchange may be an important mechanism of MB adsorption onto NWS and MWS.

4. Conclusion

On the base of the experimental results of this investigation, the following conclusion can be drawn:

- (a) Variables, influent dye concentration, flow rate, and bed depth can affect the shape of breakthrough curve.
- (b) NWS and MWS as adsorbent to remove MB from solution was proved efficiently and adsorption capacity of MWS was larger.
- (c) The Yan and BDST models adequately described the adsorption of MB onto NWS and MWS by column mode.
- (d) The exhausted column can be regenerated using 0.1 mol L^{-1} hydrogen chloride solution and reused for MB removal.

Acknowledgments

This work was supported by the National Natural Science Foundation of China for undergraduate cultivation in basic science (J0830412).

References

- [1] T. Robinson, G. McMullan, R. Marchant, P. Nigam, Remediation of dyes in textile effluent: A critical review on current treatment technologies with a proposed alternative, *Bioresour. Technol.* 77 (2001) 247–255.
- [2] Z. Aksu, Application of biosorption for the removal of organic pollutants: A review, *Process Biochem.* 40 (2005) 997–1026.
- [3] V.K. Gupta, P.J.M. Carrott, M.M.L. Ribeiro Carrott, Suhas, low cost adsorbents: Growing approach to wastewater treatment—a review, *Crit. Rev. Environ. Sci. Technol.* 39 (2009) 783–842.
- [4] V.K. Gupta, B. Gupta, A. Rastogi, S. Agarwal, A. Nayak, A comparative investigation on adsorption performances of mesoporous activated carbon prepared from waste rubber tire and activated carbon for a hazardous azo dye—Acid Blue 113, *J. Hazard. Mater.* 186 (2011) 891–901.
- [5] V.K. Gupta, B. Gupta, A. Rastogi, S. Agarwal, A. Nayak, Pesticides removal from waste water by activated carbon prepared from waste rubber tire, *Water Res.* 45 (2011) 4047–4055.
- [6] R.P. Han, Y. Wang, X. Zhao, Y.F. Wang, F.L. Xie, J.M. Cheng, M.S. Tang, Adsorption of methylene blue by phoenix tree leaf powder in a fixed-bed column: Experiments and prediction of breakthrough curves, *Desalination* 245 (2009) 284–297.
- [7] W.H. Zou, P. Han, Y.L. Li, X. Liu, X.T. He, R.P. Han, Equilibrium, kinetic and mechanism study for the adsorption of neutral red onto rice husk, *Desalin. Water Treat.* 12 (2009) 210–218.
- [8] M.C. Shih, Kinetics of the batch adsorption of methylene blue from aqueous solutions onto rice husk, effect of acid-modified process and dye concentration, *Desalin. Water Treat.* 37 (2012) 200–214.
- [9] Y. Bulut, H. Aydın, A kinetics and thermodynamics study of methylene blue adsorption on wheat shells, *Desalination* 194 (2006) 259–267.
- [10] V.K. Gupta, R. Jain, S. Varshney, Removal of Reactofix golden yellow 3 RFN from aqueous solution using wheat husk—an agricultural waste, *J. Hazard. Mater.* 142 (2007) 443–448.
- [11] R.P. Han, P. Han, Z.H. Cai, Z.H. Zhao, M.S. Tang, Kinetics and isotherms of neutral red adsorption on peanut husk, *J. Environ. Sci.* 20 (2008) 1035–1041.
- [12] V.K. Garg, M. Amita, R. Kumar, R. Gupta, Basic dye (methylene blue) removal from simulated wastewater by adsorption using Indian Rosewood sawdust: A timber industry waste, *Dyes Pigment.* 63 (2004) 243–250.
- [13] V.K. Gupta, A. Mittal, L. Kurup, J. Mittal, Process development for removal and recovery of metanil yellow by adsorption on waste materials—bottom ash and de-oiled soya, *J. Hazard. Mater.* 151 (2008) 834–845.
- [14] V.K. Gupta, A. Mittal, A. Malviya, J. Mittal, Adsorption of carmoisine a from wastewater using waste materials—bottom ash and de-oiled soya, *J. Colloid Interface Sci.* 355 (2009) 24–33.
- [15] V.K. Gupta, A. Mittal, V. Gajbe, J. Mittal, Removal and recovery of the hazardous azo dye acid orange 7 through adsorption over waste materials: Bottom ash and de-oiled soya, *Ind. Eng. Chem. Res.* 45 (2006) 1446–1453.
- [16] S.T. Ong, S.Y. Tan, E.C. Khoo, S.L. Lee, S.T. Ha, Equilibrium studies for Basic blue 3 adsorption onto durian peel (*Durio zibethinus* Murray), *Desalin. Water Treat.* 45 (2012) 161–169.
- [17] G. Crini, Non-conventional low-cost adsorbents for dye removal: A review, *Bioresour. Technol.* 97 (2006) 1061–1085.
- [18] V.K. Gupta, Suhas, application of low cost adsorbents for dye removal—a review, *J. Environ. Manage.* 90 (2009) 2313–2342.
- [19] R.P. Han, L.J. Zhang, C. Song, M.M. Zhang, H.M. Zhu, L.J. Zhang, Characterization of modified wheat straw, kinetic and equilibrium study about copper ion and methylene blue adsorption in batch mode, *Carbohydr. Polym.* 79 (2010) 1140–1149.
- [20] Y.J. Wu, L.J. Zhang, C.L. Gao, J.Y. Ma, X.H. Ma, R.P. Han, Adsorption of copper ions and methylene blue in single and binary system on wheat straw, *J. Chem. Eng. Data* 54 (2009) 3229–3234.
- [21] H.C. Thomas, Heterogeneous ion exchange in a flowing system, *J. Am. Chem. Soc.* 66 (1944) 1664–1666.
- [22] G. Yan, T. Viraraghavan, M. Chen, A new model for heavy metal removal in a biosorption column, *Adsorpt. Sci. Technol.* 19 (2001) 25–43.
- [23] J. Goel, K. Kadirvelu, C. Rajagopal, V.K. Garg, Removal of lead(II) by adsorption using treated granular activated carbon: Batch and column studies, *J. Hazard. Mater.* 125 (2005) 211–220.
- [24] R.P. Han, Y. Wang, W.H. Zou, Y.F. Wang, J. Shi, Comparison of linear and nonlinear analysis in estimating the Thomas model parameters for methylene blue adsorption onto natural zeolite in fixed-bed column, *J. Hazard. Mater.* 145 (2007) 331–335.
- [25] Y.S. Ho, W.T. Chiu, C.C. Wang, Regression analysis for the sorption isotherms of basic dyes on sugarcane dust, *Bioresour. Technol.* 96 (2005) 1285–1291.

- [26] R.P. Han, J.J. Zhang, P. Han, Y.F. Wang, Z.H. Zhao, M.S. Tang, Study of equilibrium, kinetic and thermodynamic parameters about methylene blue adsorption onto natural zeolite, *Chem. Eng. J.* 145 (2009) 496–504.
- [27] Z. Aksu, F. Gonen, Biosorption of phenol by immobilized activated sludge in a continuous packed bed: Prediction of breakthrough curves, *Process Biochem.* 39 (2004) 599–613.
- [28] J.Y. Song, W.H. Zou, Y.Y. Bian, F.Y. Su, R.P. Han, Adsorption characteristics of methylene blue by peanut husk in batch and column mode, *Desalination* 265 (2011) 119–125.
- [29] X.L. Wu, Y. Wang, J.L. Liu, J.Y. Ma, P. Han, Study of Malachite Green adsorption onto natural zeolite in fixed-bed column, *Desalin. Water Treat.* 20 (2010) 228–233.
- [30] L. Zhao, W.H. Zou, L.N. Zou, X.T. He, J.Y. Song, R.P. Han, Adsorption of methylene blue and methyl orange from aqueous solution by iron oxide-coated zeolite in fixed bed column: Predicted curves, *Desalin. Water Treat.* 22 (2010) 258–264.
- [31] R.P. Han, J.H. Zhang, W.H. Zou, H.J. Xiao, J. Shi, H.M. Liu, Biosorption of copper(II) and lead(II) from aqueous solution by chaff in a fixed-bed column, *J. Hazard. Mater.* 133 (2006) 262–268.
- [32] A. Mittal, J. Mittal, A. Malviya, D. Kaur, V.K. Gupta, Decoloration treatment of a hazardous triarylmethane dye, Light Green SF (Yellowish) by waste material adsorbents, *J. Colloid Interface Sci.* 342 (2010) 518–527.
- [33] R.P. Han, L.N. Zou, X. Zhao, Y.F. Xu, F. Xu, Y.L. Li, Y. Wang, Characterization and properties of iron oxide-coated zeolite as adsorbent for removal of copper(II) from solution in fixed bed column, *Chem. Eng. J.* 149 (2009) 123–131.
- [34] V.K. Gupta, I. Ali, V.K. Saini, Adsorption studies on the removal of Vertigo Blue49 and Orange DNA13 from aqueous solutions using carbon slurry developed from a waste material, *J. Colloid Interface Sci.* 315 (2007) 87–93.